paper on methodology

Absolute quantitation of tissue phospholipids using ^{31}P NMR spectroscopy

Kenneth R. Metz[1] and Laura K. Dunphy[2]

Department of Radiology, Deaconess Hospital and Harvard Medical School, One Deaconess Road, Boston, MA 02215

Abstract ^{31}P NMR spectroscopy has been used to quantitate phospholipids in tissue extracts without requiring their physical separation. Concentrated lipids were dissolved in chloroform–methanol–water 100:36:9 (v/v/v) containing a cesium salt of (ethylenedinitrilo)tetraacetic acid. Tri-n-butyl phosphate was added at the beginning of lipid extraction as an NMR internal standard, permitting the absolute quantitation of phospholipids in μmoles per gram of tissue. For efficient data collection, 10 mM chromium(III) acetylacetonate was included to promote relaxation. It was found that spectral peak separations could be optimized by manipulating the sample temperature. Phospholipid levels determined by NMR agreed with colorimetric measurements and literature values for rat liver and brain. Using a 0.5–1 g tissue sample and 800 averages (2 h acquisition), the coefficient of variation for total phospholipids was 2–3%.–**Metz, K. R., and L. K. Dunphy.** Absolute quantitation of tissue phospholipids using ^{31}P NMR spectroscopy. *J. Lipid Res.* 1996. **37:** 2251–2265.

Supplementary key words lipid analysis • internal standard • chemical shift • relaxation • resolution • solvent • temperature

Tissue phospholipid extracts traditionally have been analyzed by chromatography, and conditions for the separation of phospholipids by head group have become highly refined. Unfortunately, the usual chromatographic detection methods do not provide direct quantitation of the separated molecular classes. Instead, phospholipids are often measured by fraction collection, followed by digestion and phosphorus analysis using the phosphomolybdate blue colorimetric method (1). This approach is accurate and sensitive, but it is also slow and labor-intensive.

^{31}P NMR spectroscopy has emerged as an attractive alternative to chromatography for the determination of phospholipids in extracts. The principal advantages of NMR are that physical separation of the molecular classes is unnecessary and that, under proper conditions, the area of each NMR peak is directly proportional to the amount of phosphorus in the corresponding lipid. Narrow spectral lines have been obtained by incorporating the phospholipids into mixtures containing EDTA and either aqueous detergents (2–10) or organic solvents (7, 8, 11–35). The hydrated chloroform/methanol solvent system introduced by Meneses and Glonek (13) has proven particularly expeditious. We now report several improved techniques for the ^{31}P NMR analysis of phospholipids in this solvent. First, it is shown that tri-n-butyl phosphate (Bu_3PO_4) added at the beginning of the lipid extraction process may subsequently be used as an NMR internal standard, permitting the absolute quantitation of individual phospholipid classes in μmoles per gram of tissue. The spin-lattice relaxation time T_1 of Bu_3PO_4 is much longer than those of the phospholipids. Addition of the paramagnetic complex chromium(III) acetylacetonate efficiently reduces all the ^{31}P T_1 values and avoids the need to use long data collection times or saturation factors. Finally, the effect of sample temperature has been investigated and shown to be an

Abbreviations: AAPC, β-acyl-γ-O-alkylphosphatidylcholine; Bu_3PO_4, tri-n-butyl phosphate; CL, cardiolipin; $Cr(acac)_3$, chromium(III) acetylacetonate; EDTA, (ethylenedinitrilo)tetraacetate; Et_3PO_4, triethyl phosphate; FWHM, full line width at half-maximum intensity; LPC, lysophosphatidylcholine; Me_3PO_4, trimethyl phosphate; NA, number of averages; NMR, nuclear magnetic resonance; PA, phosphatidic acid; PC, phosphatidylcholine; PC plas, phosphatidylcholine plasmalogen; PE, phosphatidylethanolamine; PE plas, phosphatidylethanolamine plasmalogen; PG, phosphatidylglycerol; Ph_3PO_4, triphenyl phosphate; PI, phosphatidylinositol; PIP, phosphatidylinositol-4-phosphate; PIP_2, phosphatidylinositol-4,5-bisphosphate; ppm, parts per million; PS, phosphatidylserine; r^2, square of the correlation coefficient; s.e.m., standard error of the mean; s.d., standard deviation; SD, Sprague-Dawley; S/N, ratio of signal to root-mean-square noise; SPH, sphingomyelin; τ, NMR interpulse cycle time; T_1, NMR spin-lattice relaxation time; T_2, NMR spin-spin relaxation time; TLC, thin-layer chromatography; TMS, tetramethylsilane; U, unidentified phospholipid.

[1]To whom correspondence should be addressed.

[2]Present address: Tufts University School of Medicine, 145 Harrison Avenue, Boston, MA 02111.

effective means to optimize the separation between NMR peaks.

EXPERIMENTAL METHODS

Animals

Male laboratory rats of the Wistar Furth (WF/NHsd), Lewis (LEW/SsNHsd), ACI (ACI/SegHsd), and LBNF1 (LBNF1/Hsd) strains were obtained from Harlan Sprague-Dawley, Inc. (Indianapolis, IN). Animals were housed 2–4 to a cage at 23 ± 1°C, 50% humidity, and with a 12 h light/dark cycle. Rat chow (Prolab R-M-H 3000, Agway Inc., Syracuse, NY) and water were available ad libitum. Chow was specified by the manufacturer to contain, typically, 22.5% protein, 5.5% fat, and 4.5% fiber with gross, digestible, and metabolizable energies of 4.4, 3.7, and 3.5 kcal/g, respectively. Animals were allowed to stabilize on this diet for at least 4 days and were not fasted before use. Each rat was anesthetized with diethyl ether and the liver was removed, resulting in death by exsanguination. In some cases, the whole brain was also removed. Fast freezing to prevent the loss of polyphosphoinositides was not performed. Excised tissues were blotted and cut into ~4 mm pieces. Samples were prepared by weighing 0.5–1 g of randomized pieces into polyethylene tubes which were then flushed with nitrogen, sealed, and placed in a freezer at -70°C.

Materials

All commercial chemicals were used as received without additional purification. Methanol, chloroform, 85% H_3PO_4, $Na_2S_3O_5$, and K_2HPO_4 were A.C.S. Analytical Reagent grade obtained from Fisher Scientific, Pittsburgh, PA. Bu_3PO_4 (99+%), Me_3PO_4 (99+%), Ph_3PO_4 (99+%), $Cr(acac)_3$ (97%), $(NH_4)_6Mo_7O_{24} \cdot 4H_2O$ (A.C.S. Analytical Reagent grade), and 2,4-diaminophenol dihydrochloride (98%) were purchased from Aldrich Chemical Co., Milwaukee, WI. TMS (99.9+%), EDTA (acid form, A.C.S. Analytical Reagent grade), $CsOH \cdot H_2O$, and pure phospholipids were supplied by Sigma Chemical Co., St. Louis, MO. Dry nitrogen gas (99.998+%) was obtained from Air Products Co., Allentown, PA, and deuterochloroform (99.8%) was supplied by Cambridge Isotopes, Inc., Andover, MA. NMR tubes and spherical sample cells were manufactured by the Wilmad Glass Co., Buena, NJ.

A cesium–EDTA solution (13) was prepared by titrating an aqueous slurry of EDTA (acid form) with CsOH (aq) to pH 6.00 ± 0.04, followed by dilution to yield a final EDTA concentration of 0.2 M. The dissolved salt, containing approximately 2.3 moles of cesium per mole of EDTA, is designated as Cs-EDTA in discussions below.

Lipid extraction and colorimetric phosphorus assay

Phospholipids were extracted from rat brain and liver samples by the method of Folch, Lees, and Sloane Stanley (36). A mortar and pestle were used to grind 0.5 to 1 g of fresh or freshly thawed tissue. 5.0 ± 0.1 ml of methanol and 10.00 ± 0.03 ml of chloroform were then added. For samples used in NMR analysis, the chloroform contained an accurately known quantity of Bu_3PO_4 in the range of 320 ± 40 mg/liter. If necessary, additional methanol–chloroform 2:1 (v/v) was added to bring the total volume to 20 ml/gram of tissue. After homogenization (Brinkmann PT3000 mechanical homogenizer, 25000 rpm, 3 min) and centrifugation (DuPont Sorvall RC-5C with HS-4 bucket rotor, 1800 rpm, ~650 *g*, 6 min), the liquid was filtered through glass wool and collected. Residual tissue solids were then extracted twice more in the same manner with pure chloroform–methanol 2:1. The combined organic extracts were shaken vigorously with 0.2 volume of 0.1 M aqueous KCl for 30 s, and the liquid layers were separated by centrifugation at 1800 rpm for 30 min. The bottom layer was used for further analysis by NMR or colorimetry.

For total lipid phosphorus determination, the bottom layer was transferred quantitatively to a volumetric flask and diluted to 50 ml with chloroform–methanol 2:1; 0.25 ml of this solution was transferred to each of four test tubes and dried with nitrogen. Sample digestions and colorimetric phosphorus assays were performed according to Bartlett (1), as modified by Kates (37). Sample absorbance was determined against digested K_2HPO_4 standards using a Hewlett-Packard 8452A diode array spectrophotometer at 820 nm, the upper wavelength limit of the instrument.

NMR analysis

Samples for NMR analysis were formulated approximately as described by Meneses and Glonek (13). The total lipid extract from above was first reduced to dryness using a gentle stream of nitrogen gas. The lipids were redissolved in chloroform and 2.0 ml was placed in a 10-mm (o.d.) NMR tube; 1.08 ml of a mixture of methanol–0.2 M Cs-EDTA (aq) 4:1 (v/v) was added to the tube. This was followed by the addition of 0.40 ml of 87 mM $Cr(acac)_3$ in deuterochloroform optionally containing 4% (v/v) TMS. After capping the tube, the solution was mixed by inverting several times and venting. A colorless, aqueous layer formed rapidly above the clear, violet, organic layer. The tube contained chloroform–methanol–water in the ratio 100:36:9 (v/v/v), as well as 10 mM $Cr(acac)_3$. As the latter was insoluble in the aqueous layer (typically comprising ~5% of the total volume), its concentration in the organic layer was approximately 10.5 mM. In average lipid extract samples, the mole ratios of chloroform–methanol–water in

the bottom layer were 51.1:34.5:14.4, as measured from fully relaxed 300.5 MHz ^{1}H NMR spectra. This is near the composition recently found to yield optimum phospholipid peak separations in a single-phase ternary solvent system (35).

High-resolution ^{31}P NMR measurements were performed at 121.6 MHz using a 7.06 Tesla General Electric GN-300WB spectrometer equipped with a Cryomagnet Systems (Indianapolis, IN) 10 mm reverse probe. The use of a reverse probe (with the proton rf coil wound nearest the sample tube) resulted in a few percent ^{31}P sensitivity loss compared to standard probe configurations. Samples spinning at 14 Hz were positioned with the organic layer centered in the ^{31}P rf coil. Sample temperatures were controlled, usually at 34° or 38°C, and a deuterium field-frequency lock was used. The magnetic field homogeneity was optimized using the ^{1}H free induction decay, yielding Lorentzian line shapes and widths of approximately 1.5, 3.5, and 7 Hz for TMS, methanol methyl, and chloroform, respectively. Typical ^{31}P spectral acquisition parameters included a 16 μs (90°) rf pulse, ±215 Hz spectral width, 2K total data points, quadrature detection, 2.38 s acquisition time, 6.62 s relaxation delay, 9.00 s cycle time, 600–1000 averages, and total data collection time of 1.5–2.5 h. WALTZ-16 broadband ^{1}H decoupling (38) at 2.4 W was applied during acquisition but was turned off during the relaxation delay to avoid sample heating and nuclear Overhauser effects (39). The time-domain data set was subjected to exponential multiplication, yielding 0.5 Hz of additional Lorentzian line broadening in the frequency domain, and was zero filled to 16K points to aid accurate integration (40). The software provided with the spectrometer was used to integrate the total phospholipid versus Bu_3PO_4 peak areas. Each spectrum was processed and integrated at least four times to determine mean values. Relative areas of individual phospholipid peaks were calculated by least-squares Lorentzian line fitting using MacFID software (Tecmag, Inc., Houston, TX) running on a Power Macintosh 6100/60.

^{31}P spin-lattice relaxation times were measured by the inversion-recovery technique (41) with gated ^{1}H decoupling except where noted. The intensities of overlapping peaks were determined by Lorentzian line fitting. Samples were not degassed. One T_1 measurement was performed at 4.7 Tesla using a Bruker Biospec imaging/spectroscopy system.

High-frequency ("downfield") chemical shifts have been designated as positive. The ^{31}P shift scale was established by inserting a microsphere containing 85% H_3PO_4 into the NMR sample. Signals from H_3PO_4 (at 0 ppm), Bu_3PO_4, and PC could be observed simultaneously, and shifts for all other phospholipid peaks were obtained relative to Bu_3PO_4 or PC after the microsphere was removed. The ^{31}P shift scale obtained in this manner agreed with that calculated by the method of Edzes (42) from the measured ^{1}H resonance frequency of internal TMS. As the shift of Bu_3PO_4 was relatively insensitive to temperature variations, it was used as a secondary reference in some cases. Most individual phospholipid peaks were easily assigned by using published chemical shifts (13, 19, 22, 30) adjusted to our measured reference shift for 85% H_3PO_4. All uncertain assignments were verified by adding pure phospholipids directly to the test mixture.

The NMR signal-to-noise ratio (S/N) was calculated using the formula

$$S/N = \frac{A - B}{2 \cdot \left\{ \left[\sum_{i=1}^{n} (N_i - B)^2 \right] / n \right\}^{1/2}} \qquad Eq.\ 1)$$

where A is the maximum amplitude of the frequency-domain signal, B is the mean amplitude of the baseline, n is the number of points in the noise window, and N_i is the amplitude of each noise point. Statistical analyses were performed using the Macintosh software package SuperANOVA (Abacus Concepts, Inc., Berkeley, CA).

Step-by-step procedures for tissue extraction and analysis are available from the authors upon request.

RESULTS AND DISCUSSION

Phospholipid ^{31}P NMR chemical shifts and detection limits

Typical ^{31}P NMR spectra of tissue phospholipids are shown in **Fig. 1.** Few peaks can be resolved without ^{1}H decoupling, although resolution is adequate to produce reasonably accurate integrals for total phospholipids, PC, and Bu_3PO_4. With decoupling, the lines are clearly resolved and amenable to integration. Each of the decoupled peaks in Fig. 1 represents a unique phospholipid class with the assignment shown. Small side bands are visible near ±3.2 Hz from the center band of Bu_3PO_4 and are due to 2- and 3-bond ^{31}P–^{13}C spin-spin coupling (43). For quantitation purposes, the areas of these peaks are included in the total Bu_3PO_4 integral.

The chemical shift scale in Fig. 1 was referenced to the signal of 85% H_3PO_4 at 0 ppm. As the usual standard for high-resolution ^{31}P NMR, 85% H_3PO_4 has been adopted as the ultimate reference in virtually all published NMR studies of phospholipid composition. Despite this, however, three rather different scales have been reported. Some investigators (13, 21, 25) referenced shifts to the signal of glycerol 3-phosphorylcholine

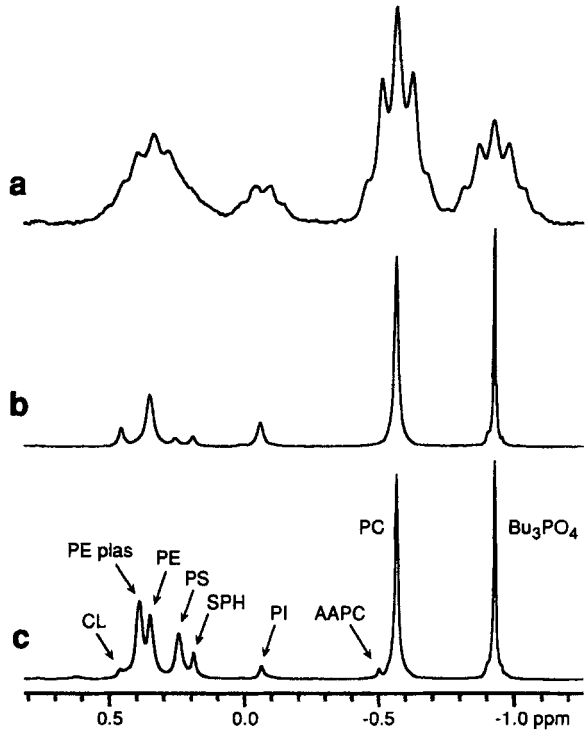

Fig. 1. ^{31}P NMR spectra (121.6 MHz) of phospholipids extracted from rat liver and brain. Spectra were acquired at 34°C, and samples contained 12.6 μmol Bu_3PO_4. Other sample preparation and data acquisition techniques are described in the Experimental Methods section. a. 0.84 g liver without proton decoupling; b. 0.84 g liver with proton decoupling; c. 0.70 g brain with proton decoupling.

added to the sample, assigning to it a chemical shift of -0.13 ppm which produced a PC shift of -0.84 ppm in chloroform–methanol–water 100:40:10. Other workers based the scale on the signal from a cell of 85% H_3PO_4 inserted into the sample. This approach yielded PC shifts of -0.51 ppm and -0.07 ppm in chloroform–methanol–water 100:22.2:6.35 and 100:37.5:12.5, respectively (19, 28). Careful measurements of the $^{31}P/^{1}H$ resonance frequency ratio for H_3PO_4 and TMS have been published, allowing the measured frequency of internal TMS to be used to establish the ^{31}P shift scale provided the value of the solvent-induced ^{1}H shift of TMS is known (22, 42). Many TMS solvent shifts have been reported, including values of +0.12 ppm (42) and +0.14 ppm (44) in chloroform. We measured solvent-induced TMS shifts by inserting a spherical cell of pure TMS into an NMR tube containing 5% (v/v) TMS dissolved in the appropriate solvent. Studies revealed little effect of temperature on the shifts between 5°C and 20°C. At 20°C, values (±0.01 ppm) of +0.14, -0.17, and -0.01 ppm were found in chloroform, methanol, and chloroform–methanol–water 100:36:9, respectively. Thus, the ternary solvent mixture induces only a very slight TMS shift to low frequency which differs from the weighted average of the shifts in chloroform and methanol. This is presumably due to the additional effect of water and, possibly, to selective solvation phenomena. By using the measured internal TMS resonance frequency in conjunction with the data of Edzes (42) and a solvent shift of -0.01 ppm, the chemical shift of PC at 34°C in the 100:36:9 ternary solvent was calculated to be -0.57 ppm. Inserting an 85% H_3PO_4 microsphere directly into our samples also gave a PC shift of -0.57 ppm, confirming the accuracy of the shift scale by two quite independent methods. Our value for the PC shift is in reasonable agreement with that of -0.51 ppm obtained in a similar solvent at room temperature by Pearce et al. (19).

The NMR detection limit (S/N = 2) for most individual phospholipids was found to be about 100 nmol (~75 μg) at 7.06 Tesla when 800 scans were averaged during a 2-h period. This value would improve slightly if a standard, instead of a reverse, probe configuration were used. The detection limit found here is similar to the value of 200 nmol reported at 1.9 Tesla using samples prepared with detergents (2). It also corresponds to the value of 25–50 μg reported with the chloroform–methanol–water system at 9.4 Tesla (27). The amount needed for quantitation obviously is greater than the detection limit, and Rana, Sultany, and Blazyk (20) have suggested a minimum of 0.5–1 mg. For the accurate determination of total phospholipids, samples containing ≥25 μmol (≥20 mg) of combined phospholipids have been found to be optimum. This quantity is contained in 0.5–1.5 g of most mammalian tissues (45). Less tissue would be needed if a higher magnetic field strength or more averages were used.

Selection of an internal standard

For practical use, an ideal internal standard would possess several properties. It should be in a convenient form, chemically inert, nonvolatile, available in high purity and at a reasonable cost. It should also produce a resonance line well resolved from the other NMR peaks but not so far removed that large spectral widths and data sets would be required. The standard should be very soluble in the chloroform–methanol 2:1 extraction solvent and should not be lost during the aqueous KCl washing step. Provided these criteria are satisfied, it should be possible to add the standard early in the extraction process so that any material losses occurring during manipulations would tend to affect both the phospholipids and the standard equally.

Several compounds have been used by other investigators as standards for absolute phospholipid quantitation, including Me_3PO_4 (7, 8, 14, 26, 34), Et_3PO_4 (46), methylenediphosphonic acid (4, 6, 10), and hexachlorocyclo-triphosphazene (9). These substances either were

TABLE 1. ^{31}P NMR spin-lattice relaxation times and line widths for rat brain and liver phospholipids at various Cr(acac)$_3$ concentrations

	^{31}P Spin-Lattice Relaxation Time T_1 (s)[a]								Typical ^{31}P Line Width (Hz)[b]							
[Cr(acac)$_3$]	CL	PE plas	PE	PS	SPH	PI	PC	Bu_3PO_4	CL	PE plas	PE	PS	SPH	PI	PC	Bu_3PO_4
mM																
0	1.47	2.56	2.45	1.88	1.94	1.51	2.67	10.3	1.1	2.3	2.1	1.9	1.6	1.7	1.0	0.3
5	1.16	1.34	1.49	1.34	1.23	1.12	1.65	2.97	1.3	2.5	2.5	2.1	2.0	2.2	1.3	0.5
10	0.91	1.12	1.17	1.03	1.16	0.92	1.36	1.83	1.7	2.6	3.0	3.5	2.0	2.4	1.4	0.6
20	0.60	0.65	0.68	0.69	0.73	0.61	0.83	0.98	1.9	3.1	4.0	3.7	2.6	2.6	2.0	1.0
30	0.48	0.59	0.56	0.58	0.60	0.53	0.65	0.65	2.2	3.5	4.2	4.2	2.9	2.9	2.2	1.3

Measurements were performed at 7.06 Tesla and 34°C using the chloroform–methanol–water 100:36:9 (v/v/v) solvent system containing Cs-EDTA.

[a] T_1 values for the overlapping peaks of CL, PE plas, PE, PS, and SPH were calculated from intensities determined by Lorentzian line fitting. Intensities for the well-resolved PI, PC, and Bu_3PO_4 lines were measured directly. Estimated T_1 uncertainties are ±10% for PE, PI, PC, and Bu_3PO_4, and ±20% for all others.

[b] Full width at half-maximum intensity, using typical shim quality. The artificial line broadening of 0.5 Hz was subtracted from all measured widths to obtain the values shown.

used as external standards or were added directly to the final sample immediately before acquiring NMR data. Instead, we sought a compound that could be incorporated into the sample at the beginning of the extraction procedure. The organophosphates Me_3PO_4, Bu_3PO_4, and Ph_3PO_4 were evaluated as potential standards. In chloroform–methanol–water 100:36:9 at 24°C, the ^{31}P chemical shifts were found to be +2.2, -0.9, and -17.7 ppm for Me_3PO_4, Bu_3PO_4, and Ph_3PO_4, respectively. The large difference between the Ph_3PO_4 shift and the phospholipid resonance region is a serious disadvantage, so this compound was not considered further. Me_3PO_4 has been especially useful as an internal standard for analyses of aqueous lipid/detergent suspensions in which it is quite soluble (7, 8, 14). Unfortunately, this high water solubility precludes its addition early in the Folch extraction process as much of the standard is lost during the aqueous washing step. Bu_3PO_4 is very soluble in chloroform but not in water, and it has a convenient chemical shift, so this compound was chosen for further testing.

To evaluate possible losses of Bu_3PO_4 during washing, 0.74 g of fresh rat liver was extracted as described in Experimental Methods using chloroform–methanol 2:1 containing 17.4 μmol of Bu_3PO_4. The decanted aqueous KCl layer was washed with 1.6 ml of pure chloroform to concentrate any Bu_3PO_4 present. The chloroform layer was isolated, and 0.6 μmol of Me_3PO_4 was added. An NMR sample containing 20 mM Cr(acac)$_3$ was then prepared from this solution using the chloroform–methanol–water 100:36:9 solvent system. A fully relaxed, ^1H-decoupled ^{31}P NMR spectrum using 6744 averages revealed only a Me_3PO_4 peak at +2.27 ppm with S/N = 56. Assuming the Me_3PO_4 and Bu_3PO_4 line widths were equal and that S/N = 2 represents the detection limit, the sample must have contained <0.021 μmol of Bu_3PO_4. Therefore, quantitation errors due to losses of Bu_3PO_4 to the wash layer should not exceed about 0.12%.

Quantitation errors would also occur if removal of solvent from the extract were accompanied by vaporization of the internal standard. Fortunately, the volatilities of organophosphate compounds are low. The manufacturer specifies the boiling point of Bu_3PO_4 as 180°C at 22 mm Hg and that of the even less volatile Ph_3PO_4 as 244°C at 10 mm Hg. To evaluate potential errors, Bu_3PO_4 losses due to evaporation were measured directly and were also compared to those of Ph_3PO_4. First, 20 ml of a chloroform solution containing 0.5 M Bu_3PO_4 and 0.5 M Ph_3PO_4 were subjected to a stream of nitrogen gas for 2.5 h, and the residue was redissolved in chloroform. ^{31}P NMR integral ratios for the two organophosphates before and after this treatment were the same within experimental uncertainty (±2%). In addition, 680 liters of nitrogen gas were blown directly onto the 8.0 cm^2 surface of 2.2 g of pure Bu_3PO_4 during a 3.0-h period. A weight loss of 0.4% occurred, yielding an upper limit for the quantitation error due to volatility of the standard. As the amount of nitrogen used was 5–10 times greater than normal, Bu_3PO_4 volatility errors for typical lipid samples are probably less than 0.1%.

Effects of NMR parameters on quantitation

The choice of NMR data acquisition parameters can profoundly affect the accuracy, precision, and efficiency with which quantitative results are obtained. To avoid using saturation factors, the phospholipid spins must be allowed to relax fully between rf pulses. Ninety-degree pulses separated by long delays are often used, but smaller nutation angles and shorter delays can also be used. Published ^{31}P NMR measurements of phospholipid composition have used nutation angles ranging from 30° to 90°. Strategies for obtaining fully relaxed, quantitative data have been investigated in considerable detail, and the use of large, instead of small, nutation angles was shown to be the most efficient method

(47–49). Consequently, 90° pulses were used throughout this work.

The time efficiency of data acquisition is controlled mainly by the relaxation properties of the sample. At 24°C, spin-lattice relaxation times for Ph_3PO_4, Bu_3PO_4, and Me_3PO_4 (100 mM each) in chloroform were found to be 8.1, 8.5, and 14 s, respectively. Thus, using Bu_3PO_4 instead of Me_3PO_4 as a standard would allow the total analysis time to be decreased by a factor of about 1.6. Sample T_1 values can be reduced further by adding a paramagnetic relaxation agent such as $Cr(acac)_3$. This compound can often promote relaxation in organic solutions without seriously degrading the spectral resolution or changing the chemical shifts (50, 51). ^{31}P nuclear spin relaxation usually occurs through the chemical shift anisotropy (CSA) and intramolecular ^1H–^{31}P dipolar (D) mechanisms (52). In the presence of a paramagnetic agent, intermolecular electron–^{31}P dipolar interactions (E) provide an additional mechanism:

$$\frac{1}{T_1^{total}} = \frac{1}{T_1^{CSA}} + \frac{1}{T_1^{D}} + \frac{1}{T_1^{E}} \qquad \textit{Eq. 2)}$$

^1H–^{31}P dipolar interactions can produce nuclear Overhauser effects (NOE) that interfere with quantitation by increasing ^{31}P peak intensities under the influence of ^1H decoupling. Phospholipid signal enhancements from this source have been reported to be 10–15% in organic solutions (12, 22, 30). As the $Cr(acac)_3$ concentration is increased, the total relaxation time may come to be dominated by T_1^E, and signal distortions due to NOE are reduced as the relative contribution of T_1^D diminishes (51, 53). Thus, adding $Cr(acac)_3$ not only speeds data acquisition but also improves the accuracy of quantitation by minimizing the NOE.

^{31}P spin-lattice relaxation times and typical line widths in phospholipid solutions are listed in **Table 1.** $Cr(acac)_3$ reduced the relaxation times, especially for Bu_3PO_4, while increasing the line widths somewhat. All ^{31}P lines shifted to high frequency by <0.02 ppm in the presence of 10 mM $Cr(acac)_3$. At higher concentrations, the T_1 values were even shorter but the resolution deteriorated noticeably and induced shifts were larger (e.g., +0.16 ppm at 30 mM). Therefore, samples routinely were formulated to contain 10 mM $Cr(acac)_3$. Adding $Cr(acac)_3$ in the absence of Bu_3PO_4 would offer little advantage as S/N gains from higher potential pulse rates would be canceled by losses due to phospholipid line broadening.

In samples containing no $Cr(acac)_3$, the T_1 values at 34°C shown in Table 1 were somewhat longer than those reported near room temperature for similar solvents and field strengths (19, 20, 22, 27). Glonek (30) has recently studied the relaxation properties of PC, finding a linear increase in T_1 with increasing temperature. **Table 2** lists T_1 values between 4° and 34°C for several prominent spectral lines in rat liver extract containing 10 mM $Cr(acac)_3$. A reduction in sample temperature increased the relaxation efficiency, potentially allowing a shorter interpulse cycle time to be used during data acquisition. The PC T_1 at 4.7 Tesla has been reported to be about 3-fold longer than at 11.75 Tesla (30), which suggests that the chemical shift anisotropy mechanism dominates PC relaxation in organic solutions free of paramagnetic materials. To test the effect of field strength on ^{31}P relaxation in Bu_3PO_4, the T_1 was measured at 4.7 and 7 Tesla in chloroform–methanol–water 100:36:9 (v/v/v) containing Cs-EDTA and 10 mM $Cr(acac)_3$. At 24°C and without proton decoupling, the T_1 values at these two field strengths were indistinguishable. This field independence in a $Cr(acac)_3$-containing sample probably results from nearly complete dominance of the electron–^{31}P dipolar relaxation mechanism operating in the extreme narrowing limit with little contribution from the CSA mechanism. Although additional measurements in stronger fields would be desirable, the preliminary data suggest this internal standard should be suitable for use with spectrometers operating at field strengths greater than 7 Tesla.

In the absence of $Cr(acac)_3$, the phospholipid line widths shown in Table 1 are in general agreement with published values (13, 19, 20, 22, 26, 27). For example, the width of 1.0 Hz for PC compares with reported values of 0.8 to 1.6 Hz (13, 19). Using 10 mM $Cr(acac)_3$, ^{31}P line widths for samples prepared from liver were slightly greater than those for brain samples. Widths for the anionic phospholipids PS, CL, and PI differed the most, while the electrically neutral species PE, PE plasmalogen, SPH, PC, and Bu_3PO_4 were less affected. Mean differences for liver versus brain were 1.0 Hz (PS), 0.9 Hz (CL), 0.5 Hz (PI and PE), 0.3 Hz (SPH and PC), and 0 Hz (PE plasmalogen and Bu_3PO_4). This trend closely resembles those reported for phospholipid binding to Ca^{2+}, Mg^{2+}, and Al^{3+} in similar solvents (18, 24). Paramagnetic cations such as Fe^{3+}, which is abundant in liver, would be especially efficient line broadening agents.

TABLE 2. Temperature dependence of ^{31}P spin-lattice relaxation times

	Spin-Lattice Relaxation Time T_1 (s; ±10%)			
Temperature (°C)	PE	PI	PC	Bu_3PO_4
4	0.81	0.54	0.87	1.18
14	0.88	0.69	1.02	1.40
24	1.05	0.74	1.19	1.62
34	1.17	0.92	1.36	1.83

Measurements were performed at 7.06 Tesla for rat liver phospholipids in chloroform–methanol–water 100:36:9 (v/v/v) containing Cs-EDTA and 10 mM $Cr(acac)_3$.

Replacing the aqueous KCl wash during Folch extraction with an aqueous EDTA wash might scavenge traces of these cations and reduce the line widths in liver samples (11, 26).

When the relaxation times are known, they can be used to predict the optimum pulse sequence cycle time for accurate quantitation. The application of a series of 90° rf pulses separated by time intervals τ produces steady-state magnetization M_τ given by (54)

$$M_\tau = M_\infty [1 - \exp(-\tau / T_1)] \qquad Eq.\ 3)$$

where M_∞ is the fully relaxed magnetization. Equation 3 assumes that all transverse magnetization disappears prior to each rf pulse and that nuclear Overhauser effects are absent. The amount of a phospholipid is calculated from the ratio of its peak area to that of the internal standard, leading to

$$\frac{M_t^P}{M_t^S} = \frac{M_\infty^P}{M_\infty^S} \cdot \left[\frac{1 - \exp(-t / T_1^P)}{1 - \exp(-t / T_1^S)} \right] \qquad Eq.\ 4)$$

where superscripts P and S refer to the phospholipid and internal standard, respectively. The ratio of fully relaxed magnetizations $M_\infty{}^P/M_\infty{}^P$ represents the true relative molar quantities of phosphorus in the lipid and the standard. Equation 4 shows that the measured steady-state magnetization ratio $M_\tau{}^P/M_\tau{}^S$ approaches the true ratio only when the exponential ratio term approaches 1. If $T_1{}^P = T_1{}^S$, then the correct ratio is obtained for any τ value, although using short values may reduce the S/N to unacceptable levels (Equation 3). For the more usual case where $T_1{}^P \neq T_1{}^S$, the true ratio is obtained only if τ is large compared to both $T_1{}^P$ and $T_1{}^S$. It is reasonable to use a long τ value to provide a substantial period of relaxation without proton decoupling, thus avoiding sample heating and nuclear Overhauser distortion of the peak areas. As each phospholipid has a unique T_1, Equation 4 also shows that any arbitrary choice of τ will yield a different error for each. To ensure accurate absolute quantitation for all the phospholipids, τ must be long enough to produce negligible error for the phospholipid having a T_1 that differs the most from that of the standard.

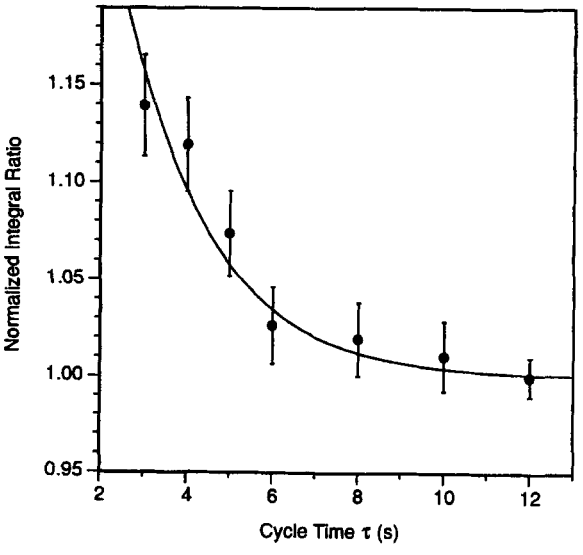

Fig. 2. Dependence of relative phospholipid integral on interpulse cycle time τ at 34°C for a mixture of rat liver and brain lipids in chloroform–methanol–water 100:36:9 (v/v/v) with Cs-EDTA and 10 mM Cr(acac)$_3$. Phospholipid integral ratios have been normalized to the value measured at τ = 12 s. Thus, the ordinate represents $(M_t{}^P/M_t{}^S)/(M_\infty{}^P/M_\infty{}^S)$. The solid line is a fit using Equation 4 and $T_1{}^P$ = 1.83 s (Table 1). The best-fit value of $T_1{}^P$ is 1.11 s (r^2 = 0.93).

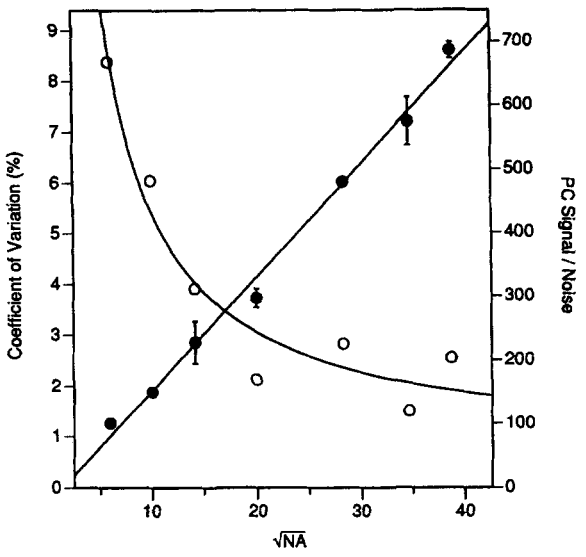

Fig. 3. Dependence of ^{31}P NMR signal-to-noise ratio (S/N) and phospholipid coefficient of variation on the number of averages NA for a 0.74 g rat liver sample. The sample contained 14.6 μmol of Bu_3PO_4 and 37.1 total μmol of phospholipid phosphorus, including 19.5 μmol of PC. Filled circles: S/N versus $\sqrt{NA}$. Open circles: coefficient of variation versus $\sqrt{NA}$. S/N was measured using the PC resonance line. Error bars represent average deviations. A fit to $S/N = a \cdot \sqrt{NA} + b$ gave a = 17.75, b = -24.99, and r^2 = 0.99. Fitting to the equation $c = (a/\sqrt{NA}) + b$, where c = coefficient of variation, gave a = 47.1, b = 0.697, and r^2 = 0.94.

Measured values of the total phospholipid integral/Bu_3PO_4 integral are plotted against cycle time τ in **Fig. 2.** All ratios were divided by the value obtained at τ = 12 s, which was assumed to represent the fully relaxed ratio $M^P{}_\infty/M^S{}_\infty$. The figure also contains a least-squares fit to Equation 4 obtained by setting $T_1{}^S$ to the measured value (Table 1) of 1.83 s and optimizing $T_1{}^P$. Agreement between theory and experiment is reasonably good (r^2 = 0.93), and the best-fit value of $T_1{}^P$ = 1.11 s falls within the phospholipid T_1 range for 10 mM Cr(acac)$_3$ in Table

TABLE 3. Total phospholipids in male rat tissues measured using ^{31}P NMR and colorimetry[a]

Tissue	Strain	Animal Wt	Total Phospholipids by NMR	Total Phospholipids by Colorimetry
		g	*μmol lipid P/g tissue ± s.d.*	
Liver	Lewis	226	47.2 ± 1.3 (4)	44.8 ± 1.2 (4)
Liver	LBNF1	454	49.9 ± 1.2 (5)	48.4 ± 1.3 (4)
Liver	ACI	253	48.7 (1)	
Liver	WF	417	45.7 ± 1.8 (4)[b] 44.9 ± 0.6 (3)[c] 46.2 ± 1.0 (4)	
Brain	ACI	203	68.02 (1)	66.07 (1)
Brain	ACI	206	67.72 (1)	67.43 (1)
Brain	ACI	210	66.45 (1)	64.39 (1)
Brain	ACI	217	71.14 (1)	69.15 (1)
Brain	ACI	218	65.37 (1)	63.40 (1)
Brain	ACI	232	62.84 (1)	60.44 (1)
Mean ± s.d.		214.3 ± 10.5	66.9 ± 2.8 (6)	65.1 ± 3.1 (6)
Brain	ACI	223	67.78 (1)	
Brain	ACI	226	70.43 (1)	
Brain	ACI	332	72.16 (1)	69.87 (1)

[a]Each row represents a single animal. Some tissues were divided to provide replicate samples, the number of which is shown in parentheses. Triple Folch extraction was used except where noted.
[b]Using single extraction.
[c]Using double extraction.

1. The absence of large differences between the data and the fit, especially for short τ values, suggests that nuclear Overhauser effects do not interfere with quantitation. Integral ratios for $\tau \geq 8$ s were statistically equivalent, so $\tau = 9$ s was chosen for subsequent work. Under these conditions, Equation 4 shows that individual sample phospholipids will be overestimated by 0.60–0.73%. Errors of this type should not exceed 1% at any temperature below about 40°C and will be even smaller at lower temperatures where T_1 values are shorter (Table 2). Although it would be possible to correct the measured peak areas for these differential saturation effects, this has not been done because the errors are well within the uncertainty of the NMR measurement (vide infra).

In addition to relaxation times, other experimental parameters affect quantitation accuracy and precision. The final integrals contain errors due to finite S/N, imperfect phasing, miscompensation for baseline drift, small variations in the amount of internal standard added, and errors in the frequency range chosen for integration. Lorentzian NMR lines contain broad wings of low intensity that must be included if accurate integrals are to be obtained (40). The PC and Bu_3PO_4 signals overlapped very slightly, and the dividing frequency for integration was defined as the local minimum between the peaks. Any reasonable choice of frequency in this region produced a variation of less than ±0.2% in the total phospholipid/Bu_3PO_4 integral ratio.

The effects of finite S/N would be expected to dominate the precision in cases where the S/N was poor. Using larger tissue samples or averaging more scans should improve the S/N, eventually to the point that other effects would begin to control the uncertainty of the measurement. To test this, the precision of total phospholipid quantitation was measured versus the number of averages (NA) using a sample prepared from 0.74 g of rat liver. Two independent ^{31}P NMR spectra were acquired for each of 7 NA values ranging from 36 to 1500. Total phospholipid and Bu_3PO_4 peaks in each spectrum were then integrated 7 times, yielding 14 integral ratio values per NA value. The S/N was also measured for PC in each spectrum. As demonstrated by **Fig. 3,** the experimental S/N showed the expected linear dependence on $\sqrt{NA}$ ($r^2 = 0.99$). The coefficient of variation (i.e., 100 × s.d./mean) for total phospholipid phosphorus decreased with increasing NA. The data were fit using the equation $c = (a/\sqrt{NA}) + b$, where c is the coefficient of variation, the ratio term represents contributions that depend inversely on S/N, and b includes random errors that are independent of S/N. The quality of the fit was reasonably good ($r^2 = 0.94$), suggesting a limiting precision of about ±2% for practical NA values. Improving the precision substantially would exact a high cost in data collection time or the amount of tissue needed. Using best-fit parameters, the model predicts that NA = 24,000 (or PC S/N = 2700) would be necessary to reduce the uncertainty to ±1% for this sample size, requiring 60 h of data collection. Alternatively, a 4-g sample could be used with NA ≈ 800. Overall, for samples containing 35–40 μmol of total

TABLE 4. Comparison of rat phospholipids measured in this work with literature values

Tissue	Strain	Age	Wt.	Total PL[a]	Method	Ref.
		wk	*g*			
Liver	SD	8	276 ± 31	55.4 ± 1.0	colorimetry	71
Liver	Donryu	8.3	315	38.2 ± 4.4	colorimetry	72
Liver	SD	10–11	374 ± 12	53.4 ± 4.1	colorimetry	71
Liver	Lewis	12	226	44.8 ± 1.2	colorimetry	this work
Liver	Lewis	12	226	47.2 ± 1.3	^{31}P NMR	this work
Liver	ACI	13	253	48.7	^{31}P NMR	this work
Liver	Wistar		~250	34.7	colorimetry	73
Liver	Wistar		275 ± 5	38.8 ± 1.9	colorimetry	74
Liver	SD	17.3	395	35.1 ± 5.4	colorimetry	75
Liver	Wistar	17–23	423 ± 40	56.1 ± 3.3	colorimetry	71
Liver	Wistar	24	~500	36.0 ± 3.4	colorimetry	65
Liver	WF	36	417	45.6 ± 1.3	^{31}P NMR	this work
Liver	SD	39	490	31.4 ± 3.1	colorimetry	75
Liver	SD	63–69	751 ± 102	54.7 ± 5.1	colorimetry	71
Liver	LBNF1	74	454	48.4 ± 1.3	colorimetry	this work
Liver	LBNF1	74	454	49.9 ± 1.2	^{31}P NMR	this work
Liver	SD	78		28.0 ± 4.5	colorimetry	75
Liver	Wistar	100–102	545 ± 63	49.2 ± 3.3	colorimetry	71
Brain	SD	8.6	222	67.6	colorimetry	67
Brain	Wistar	10		67.0	colorimetry	68
Brain	ACI	10–12	214 ± 10	65.1 ± 3.1	colorimetry	this work
Brain	ACI	10–12	217 ± 10	67.4 ± 2.7	^{31}P NMR	this work
Brain	WF	13	332	69.9	colorimetry	this work
Brain	WF	13	332	72.2	^{31}P NMR	this work
Brain	SD		300–350	73.6	colorimetry	76
Brain	SD	20.6	385	67.0	colorimetry	67
Brain	Wistar	~22		72.2	colorimetry	77
Brain	SD	25.7		69.0	colorimetry	66

[a]Total phospholipids expressed as mean μmoles lipid phosphorus/g fresh tissue ± s.d. (when known). Some values were calculated from data reported in other units by using a mean of 775 g phospholipid/mole. Uncertainties reported as ± s.e.m. were converted to standard deviations using s.d. = s.e.m. × $\sqrt{n}$, where n is the number of animals used.

phospholipids, little is gained by averaging more than about 800 scans under these conditions.

A final requirement for a suitable internal standard is inertness. To confirm the absence of slow Bu_3PO_4 hydrolysis or other deleterious reactions, total phospholipid/Bu_3PO_4 integrals were measured for two samples at a total of 19 time points from 0.5 to 89 h after preparation. Samples were stored between measurements in capped NMR tubes at room temperature and in ambient fluorescent light. The mean integral ratio decreased by about 3% near the end of the study but remained within about one standard deviation of the mean of the early measurements. Samples were clearly stable for at least 12 h and probably were unchanged for several days.

Table 3 lists total phospholipid values determined by ^{31}P NMR and colorimetry for rat liver and brain. NMR values for four different livers were in good agreement, and the NMR results agreed with the corresponding colorimetric data. Livers were large enough to provide replicate samples of essentially identical composition, which allowed the inherent precision of the techniques to be assessed. Coefficients of variation for colorimetry and NMR were equivalent, with typical values near 2.5% in agreement with Fig. 3. Individual brains were smaller than livers but were still adequate for one NMR and colorimetric assay on each organ. As a result of differences between individual animals, the brain coefficients of variation were larger than those found with single livers. For both liver and brain, the NMR values were

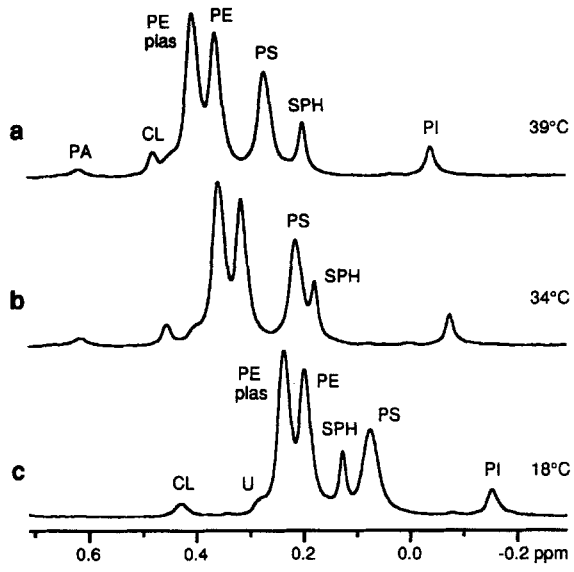

Fig. 4. Proton-decoupled ^{31}P NMR spectra of a rat brain lipid extract at three temperatures. The sample contained chloroform–methanol–water 100:36:9 (v/v/v), Cs-EDTA, and 10 mM $Cr(acac)_3$. Only the crowded spectral region near +0.3 ppm is shown; a. 39°C; b. 34°C; c. 18°C.

about 3% greater than those found by colorimetry. Up to one third of this difference can be attributed to saturation effects and preferential Bu_3PO_4 losses during solvent removal, as discussed above. Values measured by NMR are expected to be slightly higher that those from colorimetry. Incomplete release of inorganic phosphate during perchloric acid digestion (55) would cause the colorimetric values to be low. Imperfect extraction efficiency and mechanical losses would also decrease the colorimetric results. The NMR data would be less affected by mechanical losses, which would leave the lipid/internal standard ratio relatively unchanged. Despite the small difference, the agreement found for the two analytical methods is very satisfactory, and the NMR values are arguably more accurate.

Replicate samples were used to determine the effect of single, double, or triple Folch extraction on quantitation in a WF rat liver. The mean phospholipid levels found were very similar (Table 3). Multiple extraction cycles produced smaller standard deviations as these masked inconsistencies in extraction efficiency that occurred during the first cycle. Using one-factor analysis of variance followed by a post hoc Scheffe's S test, no significant differences in the means were found for different numbers of extraction cycles (smallest P = 0.46). Overall, by adding the internal standard early in the lipid extraction process, accurate phospholipid means probably can be obtained by extracting only once. However, the potential improvement in precision would often justify the small additional effort required to perform a second extraction cycle.

Table 4 compares the total phospholipid levels found here with those reported by other investigators for animals with similar ages and weights. Literature values for adult rat brain are fairly consistent and are in excellent agreement with our results. Reported phospholipid levels for liver are less reproducible, probably because variations in diet alone can produce differences exceeding a factor of two (56). Our findings are in general agreement with the published data for liver, although most literature values are about 20% lower. This is presumably a dietary effect as values for four animals fed the same diet were quite similar, NMR and colorimetry gave equivalent results for the livers in this work, and the results for brain agreed with the literature, demonstrating the absence of systematic flaws in our analytical methods.

Optimization of peak separation

As shown in Fig. 1, most phospholipid NMR peaks are not completely resolved in a 121.6 MHz spectrum. Quantitative analysis of individual phospholipids requires that accurate areas be obtained for each of these peaks. Consequently, it is important to optimize the peak separation, particularly in the relatively congested spectral region near +0.3 ppm. One way to achieve this is by manipulating the sample composition (19, 22, 33, 35). For example, the solvent polarity can be changed by varying the amounts of water or methanol relative to chloroform in the total mixture. Such changes alter the phospholipid chemical shifts, especially for PS (12, 22, 35). Unfortunately, once an NMR measurement has shown that resolution is inadequate, reformulating the sample can be inconvenient.

Several investigators (19, 21, 23, 25) have noted the importance of regulating the sample temperature to avoid broadening the phospholipid peaks, implying the chemical shifts may vary with temperature. A temperature dependence has been demonstrated for the relative shifts of egg and liver phospholipids in chloroform-methanol 2:1 (12). It therefore appeared that temperature control might provide a simple means to optimize peak separations. This is indeed the case, as shown in **Fig. 4.** All the chemical shifts varied with temperature, but that of PS was especially sensitive while the CL and SPH shifts were less affected. Through temperature control it was even possible to reverse the relative positions of the PS and SPH peaks. A change of only a few degrees can substantially improve the separation of overlapping peaks, simplifying measurements of their areas. Qualitatively, the ^{31}P shift changes that occur with increasing temperature resemble those obtained by increasing the proportions of methanol and water in the

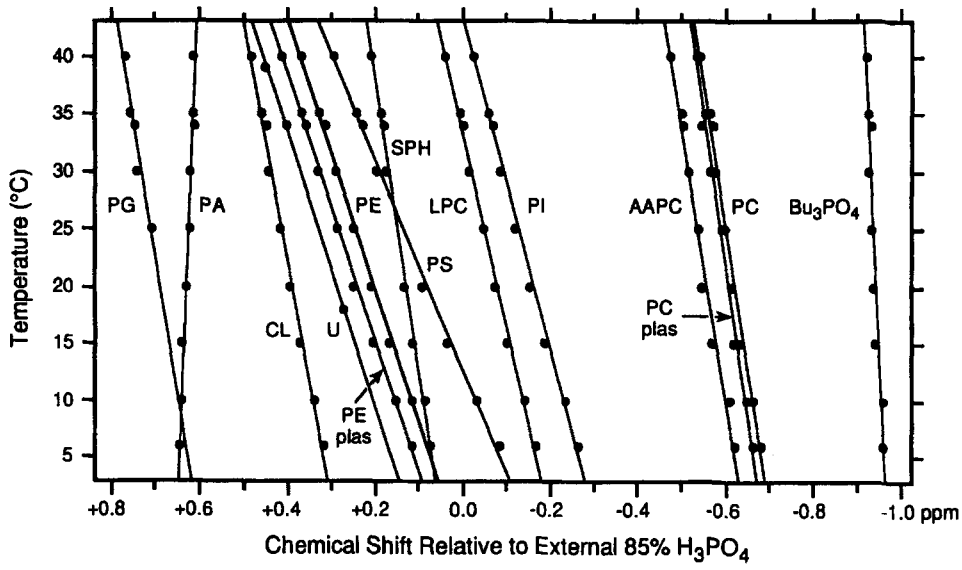

Fig. 5. ^{31}P NMR chemical shifts (δ) at various temperatures (T) for phospholipids and Bu_3PO_4 in a mixture of rat liver and brain extracts. Lipids were dissolved in chloroform–methanol–water 100:36:9 (v/v/v) with Cs-EDTA and 10 mM $Cr(acac)_3$. A microsphere of 85% H_3PO_4 inserted into the sample was used as the zero shift reference. Fitting the data to δ = a T + b gave the following best-fit values for a and b (in ppm/°C and ppm, respectively): +0.00107 and -0.961 for Bu_3PO_4; +0.00394 and -0.698 for PC; +0.00380 and -0.680 for PC plasmalogen; +0.00412 and -0.639 for AAPC; +0.00688 and -0.296 for PI; +0.00588 and -0.194 for LPC; +0.0110 and -0.138 for PS; +0.00392 and +0.0518 for SPH; +0.00852 and +0.0323 for PE; +0.00869 and +0.0694 for PE plasmalogen; +0.00851 and +0.119 for U; +0.00470 and +0.298 for CL; -0.000986 and +0.651 for PA; +0.00387 and +0.618 for

sample, although there are also important differences (12, 22, 35). Many of the improvements in peak separation that result from changing the solvent can also be achieved by means of temperature adjustments. This can be done without altering the composition of the sample or even removing it from the magnet.

The chemical shift temperature dependence was measured for a mixture of liver and brain extracts (**Fig. 5**). All the shifts varied linearly over the temperature range studied. Bu_3PO_4 showed a relatively small dependence (+0.00107 ppm/°C), making its peak at -0.94 ± 0.02 ppm useful as an internal chemical shift reference from 0°C to 40°C. Most of the phospholipid shifts were more sensitive, ranging up to +0.0110 ppm/°C for PS. The possibility that the temperature dependence resulted from thermally induced changes in solvent composition was investigated by measuring the mole percentages of chloroform, methanol, and water. As shown in **Table 5,** variations in the composition of the solvent due to temperature were insignificant and far too small to explain the effects observed here (22, 35). Hence, the phospholipid shifts reflect inherent temperature sensitivities. ^{31}P shifts to high frequency with increasing temperature have also been reported for phospholipids in micelles (3), as well as for simple phosphate esters (57), and have been attributed to small changes in the average molecular conformation about the phosphorus atom (57). The temperature dependencies of the phospholipid shifts should be useful in assigning their peaks, particularly for PS and PA.

Figure 5 shows that "windows" of optimum peak separation exist, principally near 15°C and 35°C. The temperature producing the best separation differed by a few degrees for liver and brain, probably the result of differences in bulk solvent composition due to the lipids themselves. Table 5 shows that the addition of phospholipids to the pure solvent mixture reduces the equilibrium chloroform level while increasing the proportion of water. The measured average solvent compositions of liver and brain samples differed significantly ($P < 0.02$ by Scheffe's S test), corresponding to a greater lipid concentration in the latter. Thus, a slightly different temperature was required to optimize the separation of NMR peaks for the two types of samples. This mechanism may also account for tissue and concentration dependencies in phospholipid chemical shifts reported previously (12, 13, 22). Variations in peak separation among different samples of the same type (35) were negligible, and it was not necessary to optimize the temperature for each. Despite favorable relaxation properties (Table 2), the "window" of optimum separation at 15°C was not normally used because the lines were somewhat broader, especially for PA, and the overall resolution was slightly inferior. Instead, higher

TABLE 5. Effects of temperature and lipid concentration on solvent composition for the chloroform–methanol–water 100:36:9 (v/v/v) system with Cs-EDTA and 10 mM $Cr(acac)_3$[a]

Solute	Temperature (°C)	Mole % Chloroform	Mole % Methanol	Mole % Water
None	10	53.3 ± 0.2	35.1 ± 0.2	11.6 ± 0.3
None	20	53.3 ± 0.1	34.9 ± 0.1	11.8 ± 0.2
None	30	53.0 ± 0.1	35.2 ± 0.1	11.8 ± 0.1
None	40	53.0 ± 0.2	35.8 ± 0.3	11.2 ± 0.3
30 mg PL[b]	30	52.0 ± 0.2	35.3 ± 0.1	12.7 ± 0.2
58 mg PL[b]	30	51.5 ± 0.3	35.4 ± 0.2	13.1 ± 0.3
84 mg PL[b]	30	51.4 ± 0.1	35.5 ± 0.2	13.1 ± 0.1
127 mg PL[b]	30	50.6 ± 0.2	35.3 ± 0.1	14.1 ± 0.2
Liver extract[c]	34	51.5 ± 0.8	34.3 ± 0.6	14.2 ± 0.6
Brain extract[d]	38	49.3 ± 1.5	35.7 ± 1.1	15.0 ± 0.7

[a]Actual composition of the lower layer calculated using chloroform, hydroxyl, and methyl peak integrals measured from fully relaxed ^1H NMR spectra using 5 mm tubes.

[b]Samples prepared by dissolving the indicated amount of a commercial phospholipid mixture (PL, Sigma #P-8640) in 3.48 ml of solvent. The solute contained 65% PC, 25% PE, 9% other phospholipids, 1% cholesterol, and no TLC-detectable triglycerides or free fatty acids.

[c]Mean values for 20 rat liver extract samples containing, on average, 4 mg Bu_3PO_4, 29 mg total phospholipids, and other lipids. A mean of 0.807 g of tissue was used for each sample.

[d]Mean values for 6 rat brain extract samples containing, on average, 4 mg Bu_3PO_4, 49 mg total phospholipids, and other lipids. A mean of 0.948 g of tissue was used for each sample.

temperatures were used (typically, 34°C for liver and 38°C for brain). The recent finding that ^{31}P spin-spin relaxation in PC becomes more efficient with increasing temperature (30) suggests the potential for line broadening when high temperatures are used. Line widths at 34–40°C in our samples were not noticeably greater than those at lower temperatures. This may be due to the opposing temperature effect of intermolecular ^{31}P-electron dipolar relaxation (58) in the presence of $Cr(acac)_3$. Small line width changes could also have been masked by field inhomogeneities or temperature instabilities. In any case, line broadening did not present a practical impediment to the use of temperatures up to 40°C with the samples in this study.

Relative phospholipid profiles for rat tissues determined by Lorentzian line fitting are given in **Table 6** along with literature values for animals of similar ages and weights. Mean chemical shifts are also listed, using Bu_3PO_4 as a secondary reference with δ = -0.92 ppm. Shift values for different samples and tissues agreed within ±0.02 ppm. Temperature optimization contributed to the accuracy of the line fitting process, yielding composition values and uncertainty limits in good agreement with published data for liver (59–65) and brain (5, 22, 64, 66–69). Coefficients of variation for brain were slightly greater than those for liver, a reflection of animal-to-animal variations in the former. The mole percentages found here can easily be converted to absolute quantities by multiplying by the total phospholipid values listed in Table 4. Hence, use of the internal standard allows absolute quantitation of individual, as well as total, tissue phospholipids.

Although most of the phospholipids in Table 6 can be assigned unambiguously, several are uncertain. The origins of the sharp line at -0.48 ppm and the -0.53 ppm shoulder on the PC peak are controversial. Edzes et al. (22) attributed these peaks to AAPC and PC plasmalogen, respectively, but Rana et al. (27) offered evidence that the peak at -0.48 ppm results from PC plasmalogen. The assignment shown in the table was chosen because it produced the best agreement with previous findings. Both peaks were present in spectra of brain extracts, which are known to contain AAPC and plasmalogens (64, 69). Only the -0.53 ppm peak was present in spectra of liver extracts, which contain plasmalogens (60–62) but not AAPC to our knowledge.

Two small peaks, designated as "other" in Table 6, were quantitated but not assigned. The peak labeled "U" in Figs. 4 and 5 appeared in brain samples and accounted for about 1% of the total phospholipid area. A signal in this position has been reported for several different tissues (15–17, 19, 21, 29–33) and may arise from β-acyl-γ-O-alkyl PE (22). A peak in this region has also been attributed to a derivative of SPH, possibly dihydrosphingomyelin (15, 16, 29, 30). The temperature dependence of the chemical shift for peak "U" is nearly identical to that of PE and PE plasmalogen but is quite different from that of SPH (Fig. 5), suggesting the source of this signal is β-acyl-γ-O-alkyl PE. By reducing the brain extract sample temperature to 18°C (Fig. 4c), the major

TABLE 6. Comparison of rat phospholipid distributions measured by ^{31}P NMR and chromatography[a]

		Liver	Liver	Liver	Liver	Liver	Liver	Brain	Brain	Brain
Reference		this work	this work	this work	64	65	59	this work	67	66
Strain		Lewis	WF	LBNF1	Wistar	Wistar	Wistar	ACI	SD	SD
Age (wk)		12	36	74		24		10–12	8.6	25.7
Wt (g)		226	417	454	250–300	~500		217 ± 10	222	
Phospholipid	δ (ppm)[b]	Mole % of Lipid Phosphorus								
PC	-0.57	55.8 ± 0.7	52.9 ± 1.0	52.2 ± 0.8	61.5	51.9	48.5	35.8 ± 1.0	37.5	35.7
PE	+0.37	22.2 ± 0.5	23.7 ± 0.6	24.2 ± 0.8	23.5	24.9	23.7	16.6 ± 1.3	13.9	15.5
PI	-0.04	7.5 ± 0.2	8.7 ± 0.4	8.4 ± 0.5	4.9	7.1	8.3	3.0 ± 0.2	3.9	3.2
PS	+0.28	4.4 ± 0.6	3.7 ± 0.5	4.6 ± 1.4	1.7	3.4	3.4	14.3 ± 0.6	10.7	12.3
CL	+0.47	4.1 ± 0.5	4.7 ± 0.3	4.4 ± 0.8	3.6	5.6	4.5	1.4 ± 0.2		1.7
SPH	+0.20	3.0 ± 0.1	3.3 ± 0.2	3.5 ± 0.4	4.7	4.9	4.2	4.7 ± 0.3	6.7	5.4
PG	+0.77	0.1 ± 0.1	0.4 ± 0.3	0.2 ± 0.2			0.2	0.2 ± 0.1		0.4
PA	+0.63	0.1 ± 0.1	0.1 ± 0.1	0.1 ± 0.1	0.0		0.3	1.0 ± 0.5		1.9
LPC	+0.03	0.8 ± 0.2	0.7 ± 0.2	0.5 ± 0.1	0.0	1.1	0.8	0.2 ± 0.1		
AAPC[c]	-0.48	0.0	0.0	0.0				0.8 ± 0.2		
PC plas[c]	-0.53	0.3 ± 0.2	0.6 ± 0.3	0.4 ± 0.2	0.0			0.9 ± 0.8		0.5
PE plas	+0.41	0.5 ± 0.4	0.6 ± 0.3	0.5 ± 0.3	0.0			20.0 ± 1.1		18.8
Total plas									20.0	
Other[d]		1.0 ± 0.2	0.6 ± 0.4	1.2 ± 0.6		1.0	6.5	1.0 ± 0.3	7.1	4.5

[a]Uncertainties are standard deviations. In this work, brain values are means of single measurements on 8 animals. Liver values are from 4 (Lewis), 11 (WF), and 5 (LBNF1) replicate measurements on single animals. Values in this work are from NMR, and literature results are from chromatography. Additional chromatographic values are in references 60–64, 68, and 69. Other NMR values are in references 5 and 22.

[b]Chemical shifts obtained by assigning Bu_3PO_4 δ = -0.92 ppm for all samples.

[c]Assignments of these phospholipids are uncertain (see text).

[d]"Other" phospholipids in this work yield peaks at -0.09 ppm (liver at 34°C) and +0.45 ppm (brain at 38°C).

lines shifted to reveal a trace amount of another unassigned peak at +0.34 ppm which might arise from the SPH derivative mentioned above. This suspicion is reinforced by the finding that the ^{31}P NMR spectrum of a commercial sample of bovine brain SPH, approximately 99% pure by TLC, exhibited a peak at this chemical shift accounting for about 5% of the total signal area. An additional weak unassigned line was observed in liver samples at -0.09 ppm as a low-frequency shoulder on the PI peak. A signal in this region has been attributed to sphingosylphosphorylcholine (26, 32, 33). Also, one of the two ^{31}P resonance lines of PIP apparently overlaps the PI peak (30). However, the observed peak probably does not result from PIP as rat brain contains less of this lipid than of PIP_2 (66, 70) and no measurable PIP_2 signals were found. Both PIP and PIP_2 degrade rapidly after death and neither is extracted efficiently by the Folch method (22, 70).

Summary and conclusions

Several independent techniques have been presented that enhance the ability of ^{31}P NMR spectroscopy to quantitate phospholipids in tissue extracts. Inclusion of Bu_3PO_4 as an internal standard at the beginning of the extraction process is a simple and inexpensive method for absolute quantitation. When Bu_3PO_4 is used, a relaxation agent such as $Cr(acac)_3$ should also be added to reduce the T_1 value. The accuracy and precision of quantitation can be improved by optimizing peak separations through simple temperature adjustments. This renders unnecessary many of the solvent composition changes that were required previously. The temperature dependence of the chemical shift may also prove useful for assigning peaks. Using the methods described here, ^{31}P NMR spectroscopy has been found to be accurate, versatile, and convenient for the absolute quantitation of tissue phospholipids.

This work was supported in part by an NIH Biomedical Research Support Grant.

Manuscript received 7 March 1996 and in revised form 27 June 1996.

REFERENCES

1. Bartlett, G. R. 1959. Phosphorus assay in column chromatography. *J. Biol. Chem.* **234:** 466–468.
2. London, E., and G. W. Feigenson. 1979. Phosphorus NMR analysis of phospholipids in detergents. *J. Lipid Res.* **20:** 408–412.
3. Plückthun, A., and E. A. Dennis. 1981. ^{31}P nuclear magnetic resonance study on the incorporation of monomeric phospholipids into nonionic detergent micelles. *J. Phys. Chem.* **85:** 678–683.
4. Bradamante, S., E. Barchiesi, L. Barenghi, and F. Zoppi. 1990. An alternative expeditious analysis of phospholipid composition in human blood plasma by ^{31}P NMR spectroscopy. *Anal. Biochem.* **185:** 299–303.
5. Capuani, G., T. Aureli, A. Miccheli, M. E. Di Cocco, M. T. Ramacci, and M. Delfini. 1992. Improved resolution of ^{31}P nuclear magnetic resonance spectra of phospholipids from brain. *Lipids.* **27:** 389–391.

6. Dixon, R. M., and M. Tian. 1993. Phospholipid synthesis in the lymphomatous mouse liver studied by ^{31}P nuclear magnetic resonance spectroscopy in vitro and by administration of ^{14}C-radiolabeled compounds in vivo. *Biochim. Biophys. Acta.* **1181:** 111–121.
7. Pearce, J. M., J. T. Krone, A. A. Pappas, and R. A. Komoroski. 1993. Analysis of saturated phosphatidylcholine in amniotic fluid by ^{31}P NMR. *Magn. Reson. Med.* **30:** 476–484.
8. Pearce, J. M., and R. A. Komoroski. 1993. Resolution of phospholipid molecular species by ^{31}P NMR. *Magn. Reson. Med.* **29:** 724–731.
9. Serafini, B., A. Cimini, M. Sette, and C. Sartori. 1993. ^{31}P-NMR of liver peroxisome membranes from normal and clofibrate-treated rats. *Cell. Mol. Biol.* **39:** 479–489.
10. Thomas, C. P., R. M. Dixon, M. Tian, S. A. Butler, C. J. R. Counsell, J. K. Bradley, G. E. Adams, and G. K. Radda. 1994. Phosphorus metabolism during growth of lymphoma in mouse liver: a comparison of ^{31}P magnetic resonance spectroscopy in vivo and in vitro. *Br. J. Cancer.* **69:** 633–640.
11. Henderson, T. O., T. Glonek, and T. C. Myers. 1974. Phosphorus-31 nuclear magnetic resonance spectroscopy of phospholipids. *Biochemistry.* **13:** 623–628.
12. Sotirhos, N., B. Herslöf, and L. Kenne. 1986. Quantitative analysis of phospholipids by ^{31}P-NMR. *J. Lipid Res.* **27:** 386–392.
13. Meneses, P., and T. Glonek. 1988. High resolution ^{31}P NMR of extracted phospholipids. *J. Lipid Res.* **29:** 679–689.
14. Sappey Marinier, D., R. Letoublon, and J. Delmau. 1988. Phosphorus NMR analysis of human white matter in mixed non-ionic detergent micelles. *J. Lipid Res.* **29:** 1237–1243.
15. Meneses, P., J. V. Greiner, and T. Glonek. 1990. Comparison of membrane phospholipids of the rabbit and pig crystalline lens. *Exp. Eye Res.* **50:** 235–240.
16. Merchant, T. E., J. H. Lass, M. I. Roat, D. L. Skelnik, and T. Glonek. 1990. P-31 NMR analysis of phospholipids from cultured human corneal epithelial, fibroblast and endothelial cells. *Curr. Eye Res.* **9:** 1167–1176.
17. Merchant, T. E., P. Meneses, L. W. Gierke, W. Den Otter, and T. Glonek. 1991. ^{31}P magnetic resonance phospholipid profiles of neoplastic human breast tissues. *Br. J. Cancer.* **63:** 693–698.
18. Panchalingam, K., S. Sachedina, J. W. Pettegrew, and T. Glonek. 1991. Al-ATP as an intracellular carrier of Al(III) ion. *Int. J. Biochem.* **23:** 1453–1469.
19. Pearce, J. M., M. A. Shifman, A. A. Pappas, and R. A. Komoroski. 1991. Analysis of phospholipids in human amniotic fluid by ^{31}P NMR. *Magn. Reson. Med.* **21:** 107–116.
20. Rana, F. R., C. M. Sultany, and J. Blazyk. 1991. Determination of the lipid composition of *Salmonella typhimurium* outer membranes by ^{31}P NMR. *J. Microbiol. Methods.* **14:** 41–51.
21. Sachedina, S., J. V. Greiner, and T. Glonek. 1991. Membrane phospholipids of the ocular tunica fibrosa. *Invest. Ophthalmol. Vis. Sci.* **32:** 625–632.
22. Edzes, H. T., T. Teerlink, M. S. van der Knaap, and J. Valk. 1992. Analysis of phospholipids in brain tissue by ^{31}P NMR at different compositions of the solvent system chloroform–methanol–water. *Magn. Reson. Med.* **26:** 46–59.
23. Meneses, P., and N. Navarro. 1992. ^{31}P NMR phospholipid profile of seven sea anemone species. *Comp. Biochem. Physiol.* **102B:** 403–407.
24. Merchant, T. E., and T. Glonek. 1992. ^{31}P NMR of tissue phospholipids: competition for Mg^{2+}, Ca^{2+}, Na^{+} and K^{+} cations. *Lipids.* **27:** 551–559.
25. Liang, M. T. C., T. Glonek, P. Meneses, S. J. Kopp, D. J. Paulson, L. W. Gierke, and F. N. Schwartz. 1992. NMR spectroscopy study of heart phospholipids. An exercise and anabolic steroids effect. *Int. J. Sports Med.* **13:** 417–423.
26. Meneses, P., J. N. Navarro, and T. Glonek. 1993. Algal phospholipids by ^{31}P NMR: comparing isopropanol pretreatment with simple chloroform/methanol extraction. *Int. J. Biochem.* **25:** 903–910.
27. Rana, F. R., J. S. Harwood, A. J. Mautone, and R. A. Dluhy. 1993. Identification of phosphocholine plasmalogen as a lipid component in mammalian pulmonary surfactant using high-resolution ^{31}P NMR spectroscopy. *Biochemistry.* **32:** 21–31.
28. Crans, D. C., M. Mikuš, and R. W. Marshman. 1993. ^{31}P NMR examination of phosphorus metabolites in the aqueous, acidic, and organic extracts of *Phaseolus vulgaris* seeds. *Anal. Biochem.* **209:** 85–94.
29. Driscoll, D., W. Ennis, and P. Meneses. 1994. Human sciatic nerve phospholipid profiles from non-diabetes mellitus, non-insulin-dependent diabetes mellitus and insulin-dependent diabetes mellitus individuals. A ^{31}P NMR spectroscopy study. *Int. J. Biochem.* **26:** 759–767.
30. Glonek, T. 1994. ^{31}P NMR in the analysis of extracted tissue phospholipids. *In* Phosphorus-31 NMR Spectral Properties in Compound Characterization and Structural Analysis. L. D. Quin and J. G. Verkade, editors. VCH, Deerfield Beach, Florida. 283–294.
31. Greiner, J. V., D. B. Auerbach, C. D. Leahy, and T. Glonek. 1994. Distribution of membrane phospholipids in the crystalline lens. *Invest. Ophthalmol. Vis. Sci.* **35:** 3739–3746.
32. Greiner, C. A. M., J. V. Greiner, E. Hebert, R. R. Berthiaume, and T. Glonek. 1994. Phospholipid analysis of mammalian optic nerve tissue: a ^{31}P nuclear magnetic resonance spectroscopic study. *Ophthalmic Res.* **26:** 264–274.
33. Seijo, L., T. E. Merchant, L. T. M. van der Ven, B. D. Minsky, and T. Glonek. 1994. Meningioma phospholipid profiles measured by ^{31}P nuclear magnetic resonance spectroscopy. *Lipids.* **29:** 359–364.
34. Iwata, J. L., L. G. Bardygula-Nonn, T. Glonek, and J. V. Greiner. 1995. Interspecies comparisons of lens phospholipids. *Curr. Eye Res.* **14:** 937–941.
35. Branca, M., N. Culeddu, M. Fruianu, and M. V. Serra. 1995. ^{31}P nuclear magnetic resonance analysis of phospholipids in a ternary homogeneous system. *Anal. Biochem.* **232:** 1–6.
36. Folch, J., M. Lees, and G. H. Sloane Stanley. 1957. A simple method for the isolation and purification of total lipides from animal tissues. *J. Biol. Chem.* **226:** 497–509.
37. Kates, M. 1986. Techniques of Lipidology. Elsevier, New York. 114–115.
38. Shaka, A. J., J. Keeler, T. Frenkiel, and R. Freeman. 1983. An improved sequence for broadband decoupling: WALTZ-16. *J. Magn. Reson.* **52:** 335–338.
39. Freeman, R., H. D. W. Hill, and R. Kaptein. 1972. Proton-decoupled NMR spectra of carbon-13 with the nuclear Overhauser effect suppressed. *J. Magn. Reson.* **7:** 327–329.
40. Sotak, C. H., C. L. Dumoulin, and G. C. Levy. 1984. High-accuracy quantitative analysis by ^{13}C Fourier transform NMR spectroscopy. *In* Topics in Carbon-13 NMR Spectroscopy. G. C. Levy, editor. Wiley, New York. 91–121.
41. Markley, J. L., W. J. Horsley, and M. P. Klein. 1971. Spin-lattice relaxation measurements in slowly relaxing complex spectra. *J. Chem. Phys.* **55:** 3604–3605.
42. Edzes, H. T. 1992. Determination of the resonance frequency ratio of the ^{31}P and ^{1}H NMR resonance shift standards 85% orthophosphoric acid and tetramethylsilane. *Magn. Reson. Chem.* **30:** 850–854.
43. Weigert, F. J., and J. D. Roberts. 1973. Nuclear magnetic resonance spectroscopy. Spin-spin coupling of carbon to phosphorus, mercury, nitrogen, and other elements. *Inorg. Chem.* **12:** 313–316.

44. Bacon, M. R., and G. E. Maciel. 1973. Solvent effects on the five shielding constants in tetramethylsilane and cyclohexane. *J. Am. Chem. Soc.* **95:** 2413–2426.
45. White, D. A. 1973. The phospholipid composition of mammalian tissues. *In* Form and Function of Phospholipids. G. B. Ansell, J. N. Hawthorne, and R. M. C. Dawson, editors. Elsevier Scientific Publishing Co., New York. 441–482.
46. Kriat, M., J. Vion-Dury, S. Confort-Gouny, R. Favre, P. Viout, M. Sciaky, H. Sari, and P. J. Cozzone. 1993. Analysis of plasma lipids by NMR spectroscopy: application to modifications induced by malignant tumors. *J. Lipid Res.* **34:** 1009–1019.
47. Gillet, S., and J-J. Delpuech. 1980. Optimum conditions for nondestructive quantitative analysis by carbon-13 NMR. *J. Magn. Reson.* **38:** 433–445.
48. Cookson, D. J., and B. E. Smith. 1982. Optimal experimental parameters for quantitative pulse Fourier transform proton nuclear magnetic resonance spectrometry. *Anal. Chem.* **54:** 2591–2593.
49. Cookson, D. J., and B. E. Smith. 1984. Optimal conditions for obtaining quantitative ^{13}C NMR data. *J. Magn. Reson.* **57:** 355–368.
50. Gansow, O., A. R. Burke, and G. N. La Mar. 1972. A shiftless relaxation reagent for carbon-13 magnetic resonance of organometallic carbonyl compounds. *J. C. S. Chem. Comm.* 456–457.
51. Levy, G. C., and R. A. Komoroski. 1974. Paramagnetic relaxation reagents. Alternatives or complements to lanthanide shift reagents in nuclear magnetic resonance spectral analysis. *J. Am. Chem. Soc.* **96:** 678–681.
52. James, T. L. 1984. Relaxation behavior of nucleic acids: dynamics and structure. *In* Phosphorus-31 NMR: Principles and Applications. D. G. Gorenstein, editor. Academic Press, Orlando, FL. 349–400.
53. Levy, G. C., and U. Edlund. 1975. Quantitative carbon-13 Fourier transform nuclear magnetic resonance. Limitations of spin relaxation reagents. *J. Am. Chem. Soc.* **97:** 4482–4485.
54. Freeman, R., and H. D. W. Hill. 1971. Fourier transform study of NMR spin-lattice relaxation by "progressive saturation." *J. Chem. Phys.* **54:** 3367–3377.
55. Kirkpatrick, D. S., and S. H. Bishop. 1971. Simplified wet ash procedure for total phosphorus analysis of organophosphonates in biological samples. *Anal. Chem.* **43:** 1707–1709.
56. Kosterlitz, H. W. 1958. Chemical reference substances. *In* Liver Function, R. W. Brauer, editor. American Institute of Biological Sciences, Washington, DC. 23–42.
57. Gorenstein, D. G. 1984. Phosphorus-31 chemical shifts: principles and empirical observations. *In* Phosphorus-31 NMR: Principles and Applications. D. G. Gorenstein, editor. Academic Press, Orlando, FL. 9–36.
58. Carrington, A., and A. D. McLachlan. 1979. Introduction to Magnetic Resonance. Chapman and Hall, London. 225–229.
59. Rouser, G., G. Simon, and G. Kritchevsky. 1969. Species variations in phospholipid class distribution of organs: I. Kidney, liver and spleen. *Lipids.* **4:** 599–606.
60. Gurr, M. I., J. B. Finean, and J. N. Hawthorne. 1963. The phospholipids of liver-cell fractions. I. The phospholipid composition of the liver-cell nucleus. *Biochim. Biophys. Acta.* **70:** 406–416.
61. Gurr, M. I., C. Prottey, and J. N. Hawthorne. 1965. The phospholipids of liver-cell fractions. II. Incorporation of [^{32}P]orthophosphate in vivo in normal and regenerating rat liver. *Biochim. Biophys. Acta.* **106:** 357–370.
62. Getz, G. S., W. Bartley, D. Lurie, and B. M. Notton. 1968. The phospholipids of various sheep organs, rat liver and of their subcellular fractions. *Biochim. Biophys. Acta.* **152:** 325–339.
63. Patton, G. M., J. M. Fasulo, and S. J. Robins. 1982. Separation of phospholipids and individual molecular species of phospholipids by high-performance liquid chromatography. *J. Lipid Res.* **23:** 190–196.
64. Diagne, A., J. Fauvel, M. Record, H. Chap, and L. Douste-Blazy. 1984. Studies on ether phospholipids. II. Comparative composition of various tissues from human, rat and guinea pig. *Biochim. Biophys. Acta.* **793:** 221–231.
65. Mlekusch, W., C. Celedin, R. C. Aloia, and R. Moller. 1993. Effect of a high fat diet on phospholipid class distribution and fatty acid composition in rat liver. *Int. J. Biochem.* **25:** 1539–1547.
66. Wells, M. A., and J. C. Dittmer. 1967. A comprehensive study of the postnatal changes in the concentration of the lipids of developing rat brain. *Biochemistry.* **6:** 3169–3174.
67. Norton, W. T., and S. E. Poduslo. 1973. Myelination in rat brain: changes in myelin composition during brain maturation. *J. Neurochem.* **21:** 759–773.
68. Cuzner, M. L., and A. N. Davison. 1968. The lipid composition of rat brain myelin and subcellular fractions during development. *Biochem. J.* **106:** 29–34.
69. Clarke, N. G., and R. M. C. Dawson. 1981. Alkaline $O \rightarrow N$-transacylation. A new method for the quantitative deacylation of phospholipids. *Biochem. J.* **195:** 301–306.
70. Dawson, R. M. C., and J. Eichberg. 1965. Diphosphoinositide and triphosphoinositide in animal tissues. Extraction, estimation and changes post mortem. *Biochem. J.* **96:** 634–643.
71. Uchida, K., Y. Nomura, M. Kadowaki, H. Takase, K. Takano, and N. Takeuchi. 1978. Age-related changes in cholesterol and bile acid metabolism in rats. *J. Lipid Res.* **19:** 544–552.
72. Kawasaki, M., K. Yagasaki, Y. Miura, and R. Funabiki. 1995. Reduction of hyperlipidemia in hepatoma-bearing rats by dietary fish oil. *Lipids.* **30:** 431–436.
73. Biezenski, J. J., and T. H. Spaet. 1961. Phospholipid content of subcellular fractions in adult rat organs. *Biochim. Biophys. Acta.* **51:** 221–226.
74. Chautan, M., J. Leonardi, R. Calaf, P. Lechene, R. Grataroli, H. Portugal, A-M. Pauli, H. Lafont, and G. Nalbone. 1992. Heart and liver membrane phospholipid homeostasis during acute administration of various antitumoral drugs to the rat. *Biochem. Pharmacol.* **44:** 1139–1147.
75. Carlson, L. A., S. O. Fröberg, and E. R. Nye. 1968. Effect of age on blood and tissue lipid levels in the male rat. *Gerontologica.* **14:** 65–79.
76. Spence, M. W., and L. S. Wolfe. 1967. Gangliosides in developing rat brain. Isolation and composition of subcellular membranes enriched in gangliosides. *Can. J. Biochem.* **45:** 671–688.
77. Freysz, L., R. Bieth, and P. Mandel. 1966. Les inositolphosphatides du cerveau de rat au cours de la croissance postnatale. *Bull. Soc. Chim. Biol.* **48:** 287–293.